Materials Research Proceedings **8** (2018) 18-27 doi: http://dx.doi.org/10.21741/9781945291999-3

Reactive mechanical milling of Fe-Ni-Fe_2O_3 mixtures

Traian Florin MARINCA [1,a *], Horea Florin CHICINAȘ[1,b], Bogdan Viorel NEAMȚU [1,c], Florin POPA [1,d], Niculina Argentina SECHEL [1,e] and Ionel CHICINAȘ [1,f]

[1]Materials Science and Engineering Department, Technical University of Cluj-Napoca, 103-105 Muncii Avenue, 400641 Cluj-Napoca, Romania

[a] traian.marinca@stm.utcluj.ro, [b]horea.chicinas@stm.utcluj.ro, [c]bogdan.neamtu@stm.utcluj.ro, [d]florin.popa@stm.utcluj.ro, [e]niculina.sechel@stm.utcluj.ro, [c]ionel.chicinas@stm.utcluj.ro

* traian.marinca@stm.utcluj.ro

Keywords: Reactive mechanical milling, Magnetic composite, Ferrite, Magnetite.

Abstract. Fe-Ni-Fe_2O_3 mixture in various ratios has been milled in a high energy mill for synthesis of Ni_3Fe/Fe_3O_4 type magnetic nanocomposite up to 10 h. The samples have been investigated in the light of X-ray diffraction, scanning electron microscopy, energy dispersive X-ray spectrometry and laser particle size analysis. The formation of the composite begins after 2 h of milling. After 10 h of milling the nanocomposite with the high amount of metallic phase consists in a mixture of Ni_3Fe and Fe_3O_4 alongside of a small amount of residual Fe_2O_3. Both phases are formed progressively upon increasing the milling time. Upon increasing the amount of oxide in the starting mixture at the end of the milling time the phases present in the nanocomposite material are changing. In the sample with the higher amount of oxide at the end of the milling time are present: Fe_3O_4, fcc Ni-based structure and unreacted Fe_2O_3 and Fe phases. The mean crystallite size estimated for the main phases of the nanocomposite, Ni_3Fe and Fe_3O_4, are in the nanometric range at the end of milling time independent on starting ratio among starting materials. For both, Ni_3Fe and Fe_3O_4, the mean crystallite size is ranging from 9 to 12 nm for all compositions. The nanocomposite particles shape is irregular. The powder consists in two types of particles: very fine particles with the size of less than 100 nm and larger particles with the size of a few micrometers. The micrometric particles are formed by fine agglomerated particles and by smaller particles that are welded together. The median diameter d_{50} present a significant increase in the first stage of milling and is maintained at values close to 5 μm, having small variations on each milling time.

Introduction

The development of the magnetic materials is in growth due to the large demand from various industry branches such as telecommunication, computer technologies or electronics. Therefore the development of performant magnetic materials is one of the most important and interesting research subjects [1-4]. The spinel ferrites are one the most important class of magnetic materials with a large field of applications. The ferrites are used, for example, in high frequencies applications due to their high electrical resistivity. One of the main drawbacks of the spinel ferrites when are used in high frequencies applications is the relatively low magnetic induction and magnetic permeability [5-9]. The Fe-Ni alloys have very good magnetic induction and permeability and are used nowadays in multiple applications. The use in high frequencies applications of these alloys is limited do to their low electrical resistivity as compared to the ferrites one which favour the increase of the eddy currents [10 - 12]. The synthesis of a composite

material consisting in two phases, one of Ni-Fe alloy and other in spinel ferrite can combine the above maintained advantages of each phase.

The paper presents the synthesis of composite magnetic material of Ni_3Fe/Fe_3O_4 type. The main purpose for the synthesis of this type of magnetic composite is obtain an material that can combine the high magnetic permeability of the Permalloy with the high electrical resistivity of the magnetite (electrical resistivity of magnetite is with three order of magnitude higher than the one of iron) using accessible precursors. The paper is focus on the synthesis conditions in order to obtain such type of composites.

Experimental details

As raw materials have been used Ni carbonyl, Fe NC100.24 and Fe_2O_3 powders. The ratio among the initial powder was calculated in order to correspond to fourth atom/molecule ratio between metal (both Ni and Fe) and oxide (Fe_2O_3) as follow: 0.9/0.1, 0.8/0.2, 0.7/0.3 and 0.6/0.4. These ratios correspond to the reaction of the starting materials in order to obtain Ni_3Fe and Fe_3O_4 in the following mole ratios: 100/8.5 (noted S1), 100/20 (noted S2), 100/36 (noted S3) and 100/60 (noted S4). In the above mentioned ratios the mixture has been milled in a planetary ball mill Pulverisette 4 manufactured by Fritsch up to 10 h using air as milling atmosphere. An amount of 100 g of powder has been loaded in a 500 cm^3 hardened steel vial alongside of 80 balls of 14 mm in diameter. The ball to powder mass ratio (BPR) was 9:1. The vial speed was set to 800 rpm and the disc speed was set to 400 rpm. The vial and disc were rotated in the opposite directions. The milled powders structural evolution was checked by X-ray diffraction (XRD). An INEL EQUINOX 3000 diffractometer that use CoKα radiation (λ= 1.7903 Å) was used. The investigated angular interval was 20-110°. The mean crystallite size was estimated using Scherrer formula [14]. The morphology of the powder was studied by scanning electron microscopy using a JEOL JSM-5600LV scanning electron microscope (SEM). The local chemical homogeneity was verified by energy dispersive X-ray spectrometry (EDX) using an Oxford Instrument EDX detector (INCA 200 software) with which it is equipped above mentioned scanning electron microscope. By a Laser Particle Size Analyzer (Fritsch Analysette 22—Nanotec) the samples particle size distribution and d_{50} parameter (the diameter for which 50 vol.% of particles are smaller than the d_{50} value) were studied. Before analysis an ultrasound treatment was applied for deagglomeration and dispersion of the particles.

Results and Discussion

In Fig. 1 are presented the X-ray diffraction patterns of the Fe_2O_3+Fe+Ni mixture milled for 0, 0.5, 1, 2, 3, 4, 6 and 10 h for S1. The positions of the peaks of each phase that was observed in the samples are indicated on the graph alongside of the Miller indices of the diffraction planes. It can be noticed in the patterns of the unmilled samples (0 min MM) the peaks characteristic of the Fe bcc structure from space group Im-3m (JCPDS file no. 06-0696), Ni fcc structure from space group Fm-3m (JCPDS file no. 04-0850) and Fe_2O_3 rhombohedral structure from space group R-3c (JCPDS file no. 33-0664). After only 0.5 h of milling it can observed that the diffraction peaks becomes broadened, especially the peaks of iron oxide-hematite. The stresses induced in material and the decrease of the crystallite size are the causes of the peaks broadening. Due to the fragile character of the hematite its peaks are broader as compared with the diffraction peaks of Ni and Fe. After 2 h of milling one can observe is that the change in the intensity of the peaks of iron oxide – Fe_2O_3. The diffraction plane (104) and (110), which are the most intense ones, are changing the intensity. Before milling the (104) reflection is the most intense and after 2 h of milling the (110) reflection becomes the most intense. The (110) diffraction line of Fe_2O_3 is overlapping on the (311) diffraction line of magnetite – Fe_3O_4 (JCPDS file no. 19-0629). Upon

increasing the milling time the most intense peak of hematite – (104) becomes less and less intense and the other diffraction peaks are vanishing. After 10 h of milling it is hardly identifiably hematite (104) diffraction line (the most intense peak of this phase). This indicates the progressive formation of magnetite upon increasing the milling time [9, 14].

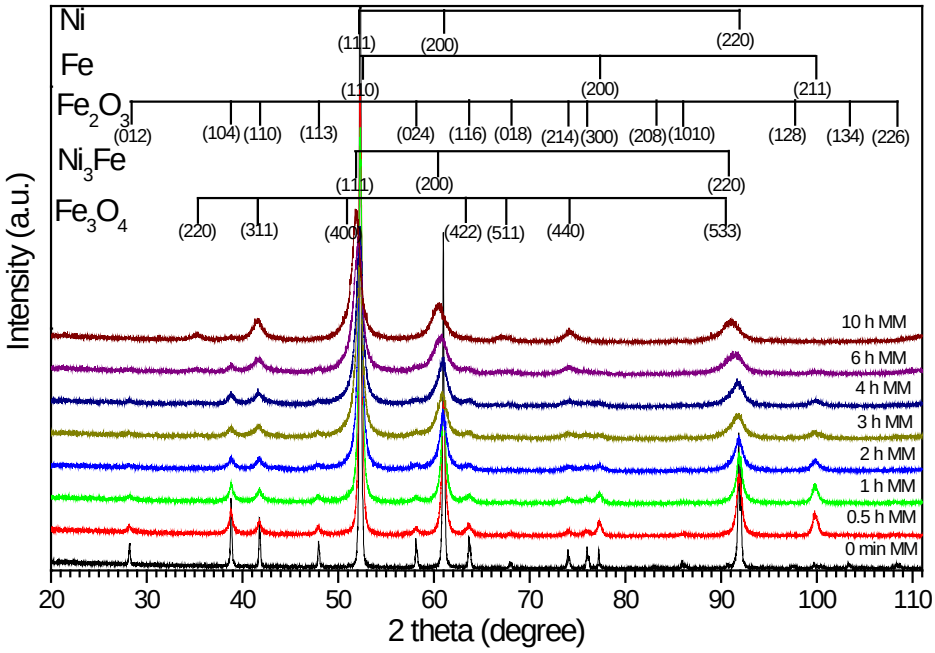

Fig.1. X-ray diffraction patterns of the Fe_2O_3+Fe+Ni mixture milled for 0, 0.5, 1, 2, 3, 4, 6 and 10 h for S1.

The iron diffraction lines becomes broadened, decreasing in intensity upon increasing the milling time and are vanishing after 10 h of milling. The Ni diffraction lines become broadened and are shifted to lower angles upon increasing the milling time. This indicates the presence of the fcc structure in material for each milling time. The displacement to lower angles of the fcc structure corroborated with the disappearance of the Fe diffraction lines is assigned to the formation of a Ni-Fe alloy. The alloy is identified as being of Ni_3Fe type (JCPDS file no. 65-3244) taken in consideration the ratio among the atoms in the starting mixture and the formation of Fe_3O_4 during milling. The Ni_3Fe is progressively form as the Fe_3O_4 and the formation of this alloy is evidenced in the Fig. 2. At the end of milling time for this composition the material consists in Ni_3Fe and Fe_3O_4 alongside to very small amount of a residual Fe_2O_3 phase. The X-ray diffraction patterns of the Fe_2O_3+Fe+Ni mixture milled for 0, 0.5, 1, 2, 3, 4, 6 and 10 h for S2 have been presented elsewhere [14]. In the case of this ratio between the starting powders it was observed the similar behaviour as in the case of S1. Although are some differences: at the end of milling time the presence of Fe_2O_3 is much more pregnant as compared to S1 and due to the larger amount of oxide the magnetite diffraction peaks are more visible in the diffraction pattern as compared to the one of Ni_3Fe.

In Fig. 3 are presented the X-ray diffraction patterns of the Fe_2O_3+Fe+Ni mixture milled for 0, 0.5, 1, 2, 3, 4, 6 and 10 h for S3. In the case of this mixture the phases that are identified at the end of milling time are in part similar with the ones observed in the case of the other two presented above. Due to the presence in the starting mixture of a larger amount of oxides thus resulting in a

Materials Research Proceedings **8** (2018) 18-27 doi: http://dx.doi.org/10.21741/9781945291999-3

larger amount of oxide also at the end of milling time and the Bragg reflections of these are better defined as compared to the other. The phases present in material at the end of milling time are: Fe_3O_4, Fe_2O_3 (larger amount as compared to S1 and S2), fcc Ni-based structure and residual Fe. It can be observed that in this case fcc structure does not have the composition closer to the one of the Ni_3Fe intermetallic compound as in the case of the other two compositions. The proves are the very low displacement of the Ni diffraction peaks to lower angles which can be assigned to the internal stress induced by milling and the presence of the residual Fe.

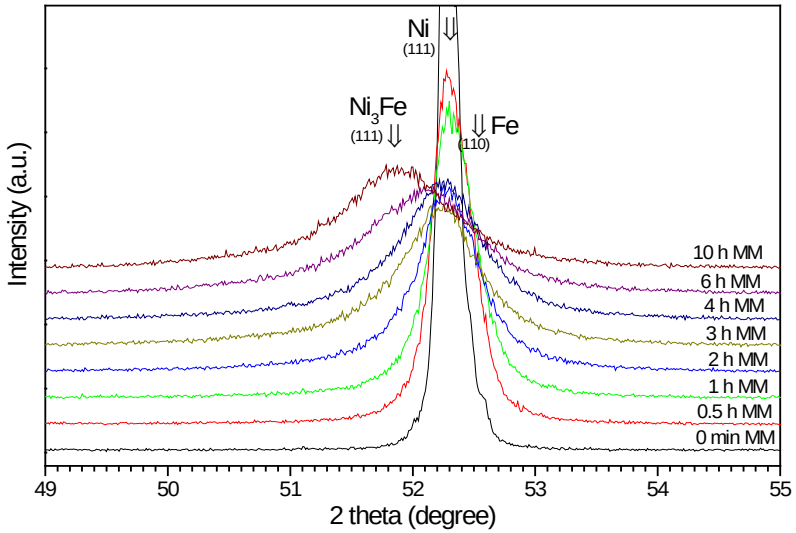

Fig. 2. Detail of the X-ray diffraction patterns of the Fe_2O_3+Fe+Ni mixture milled for 0, 0.5, 1, 2, 3, 4, 6 and 10 h for x=S1 in the zone of the most intense diffraction peaks of the newly formed Ni_3Fe compound.

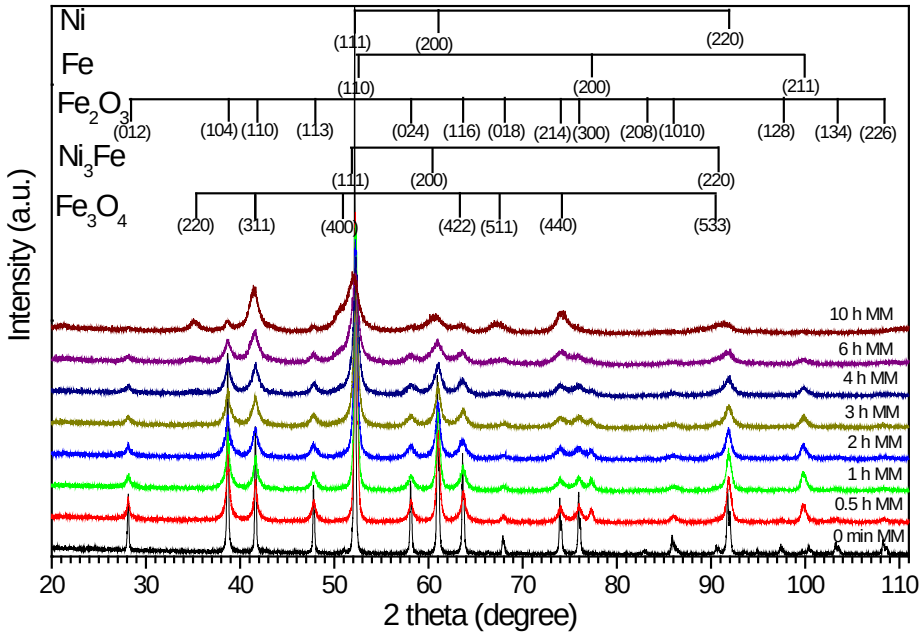

Fig. 3. X-ray diffraction patterns of the Fe_2O_3+Fe+Ni mixture milled for 0, 0.5, 1, 2, 3, 4, 6 and 10 h for S3.

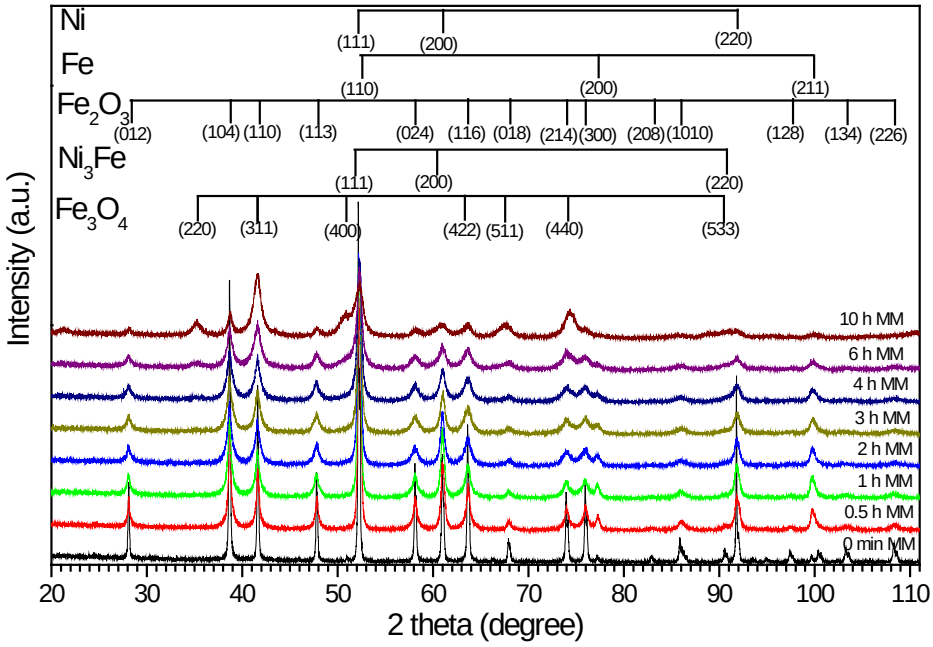

Fig. 4. X-ray diffraction patterns of the Fe_2O_3+Fe+Ni mixture milled for 0, 0.5, 1, 2, 3, 4, 6 and 10 h for S4.

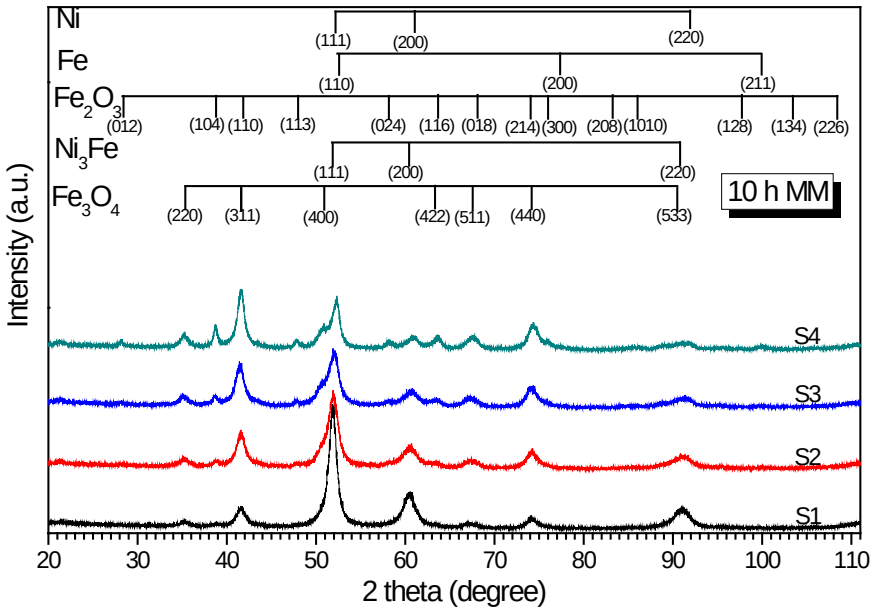

Fig. 5. X-ray diffraction patterns of the Fe_2O_3+Fe+Ni mixtures milled for 10 h for S1, S2, S3 and S4.

Fig. 4 presents the X-ray diffraction patterns of the Fe_2O_3+Fe+Ni mixture milled for 0, 0.5, 1, 2, 3, 4, 6 and 10 h for S4. The phases identified in the diffraction patterns are similar with the ones identified in the case of the samples S3. For a better view of the difference between the phases present in the samples S1, S2, S3 and S4 after 10 h of milling the X-ray diffraction patterns are presented in the Fig. 5.

Materials Research Proceedings **8** (2018) 18-27 doi: http://dx.doi.org/10.21741/9781945291999-3

Table 1. Mean crystallite size of the Ni_3Fe and Fe_3O_4 after 10 h of milling for samples S1, S2, S3 and S4.

Phase	Crystallite size (nm)			
	S1	**S2**	**S3**	**S4**
Ni_3Fe	11	9	10	12
Fe_3O_4	9	10	10	12

In the case of each composition the phases are in nanocrystalline state and the powder is a nanocomposite one of Ni_3Fe/Fe_3O_4 type. In the table 1 are presented the mean crystallite size of the Ni_3Fe and Fe_3O_4 (main phases of the composite) after 10 h of milling for samples S1, S2, S3 and S4. One can observe for both phases is the mean crystallite size ranging from 9 to 12 nm for all four compositions. The width of the diffraction peaks is increasing upon increasing the milling time this indicating a decrease of the crystallite size upon increasing the milling time for both phases (metallic and oxide) and increasing of the internal stresses. The crystallite size decreasing upon increasing the milling time is in good relation with the earlier reported results both on ferrites and Ni-based alloys [11, 14-16].

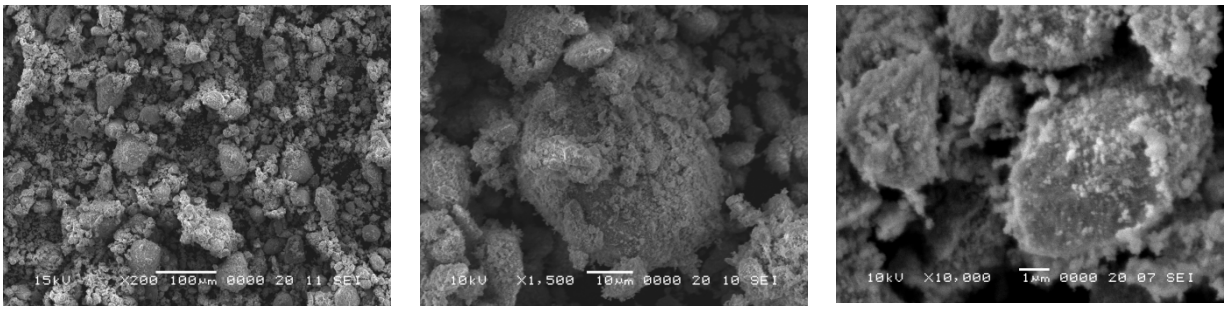

Fig. 6. SEM images of a sample milled for 1h for the composition S3 at magnification of 200x, 1500x and 10,000x.

Fig. 6 shows the SEM images of a sample milled for 1h for the composition S3 at three magnifications: 200x, 1500x and 10,000x. The particles shape is irregular. At a first look it can be remarked two types of particles: very fine particles with the size of less than 100 nm and larger particles with the size of a few micrometers. At a closer look it can be remarked that the micrometric particles are formed by fine agglomerated particles and by small particles that are welded together upon processing the powder in the mill.

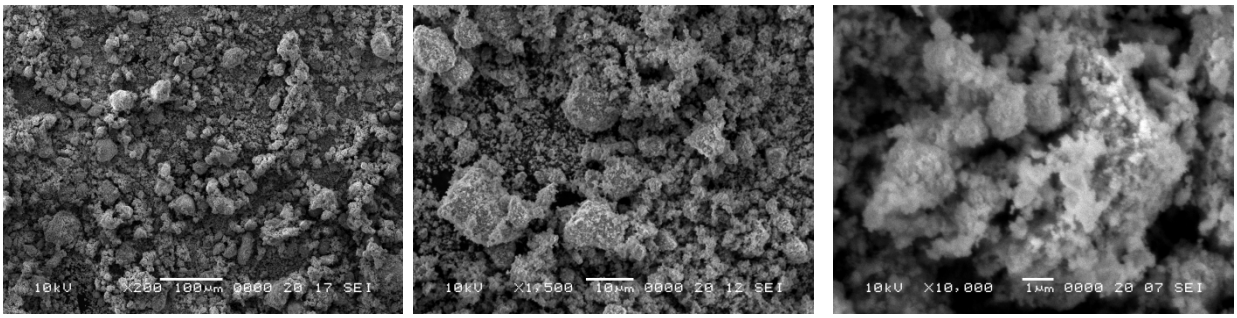

Fig. 7. SEM images of a sample milled for 3h for the composition S3 at magnification of 200x, 1500x and 10,000x.

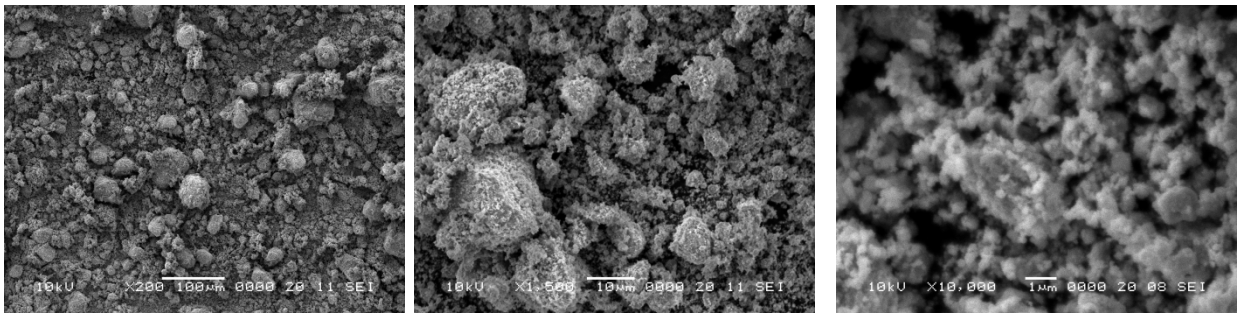

Fig. 8. SEM images of a sample milled for 6h for the composition S3 at magnification of 200x, 1500x and 10,000x.

SEM images of a sample milled for 3h for the composition S3 at magnification of 200x, 1500x and 10,000x are presented in Fig. 7. The powder morphology does not present significant change upon increasing milling time from 1h to 3h. Also after 6h of milling the powder present similar characteristics as in the case of the powder milled for smaller milling time. In Fig. 8 are displayed SEM images of the sample milled for 6h for the composition S3 at magnification of 200x, 1500x and 10,000x.

The EDX local chemical elemental mapping for a sample milled for 6 h from the composition S3 is revealed in the Fig. 9. The Ni, Fe and O elements are uniformly distributed in the analysed sample. This suggests a very fine distribution of the metallic and oxide phases. This type of investigation comes to confirm the formation of the nanocomposite by mechanical milling by formation of an intimate mixture between the metallic phase and oxide phase at nanoscale.

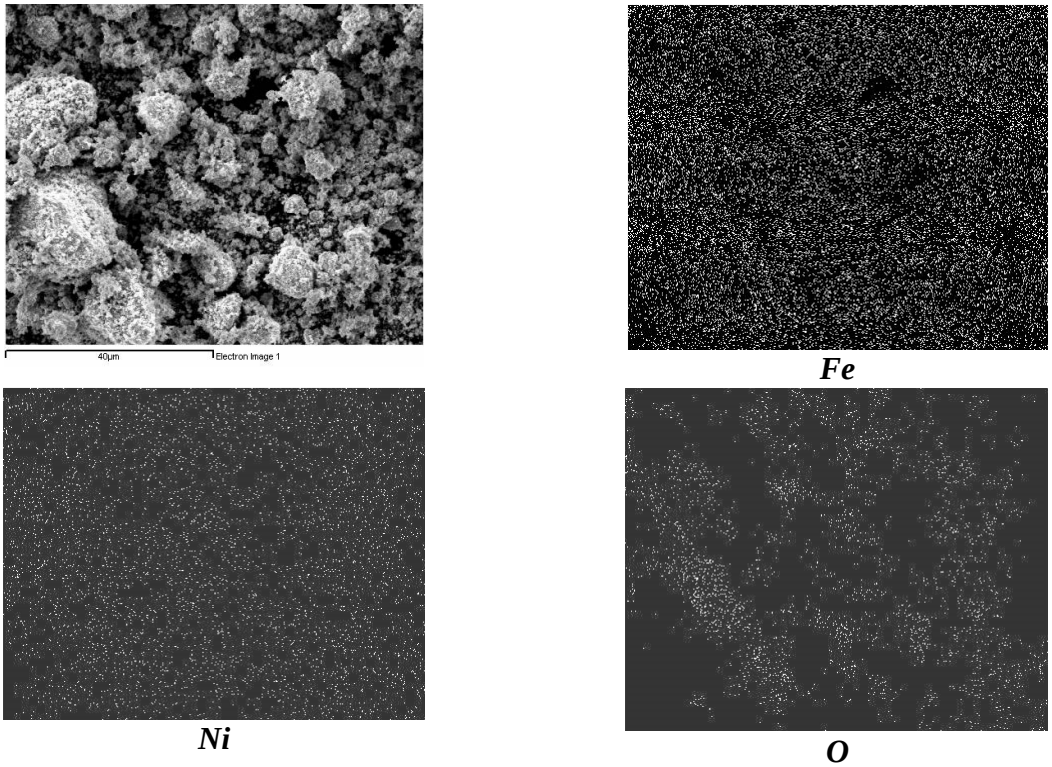

Fig. 9. EDX local chemical elemental mapping for a sample milled for 6 h from the composition S3.

Materials Research Proceedings **8** (2018) 18-27 doi: http://dx.doi.org/10.21741/9781945291999-3

The evolution of the d_{50} parameter as a function of the milling time for the S2 samples as it results from the particle size analysis effectuated with the laser particle size analyser is displayed in Fig. 10. It can be observed that the starting sample presents a median diameter less than 1 micrometer. This is due to the very fine particles of Ni and Fe_2O_3 present in the starting mixture. The iron particles are larger as compared to the ones of Ni and Fe_2O_3 but due to the low amount in this composition it does not influence in deep the median size of the particles of the starting mixture. On can note after 0.5h of milling a large increase of the median diameter occurs up to about 8 μm. This is assigned to the cold welding of the particles in the early stage of mechanical milling [16]. Increasing the milling time at 1h leads to a decrease of the median diameter up to around 5 μm. This decrease is assigned to the formation of the intimate mixture between the oxide and metallic phase which creates composite particles and which becomes more fragile due to the presence of oxide. Increasing the milling time up to 10 h of milling keeps the median diameter close to the value of 5 μm, having small variations on each milling time.

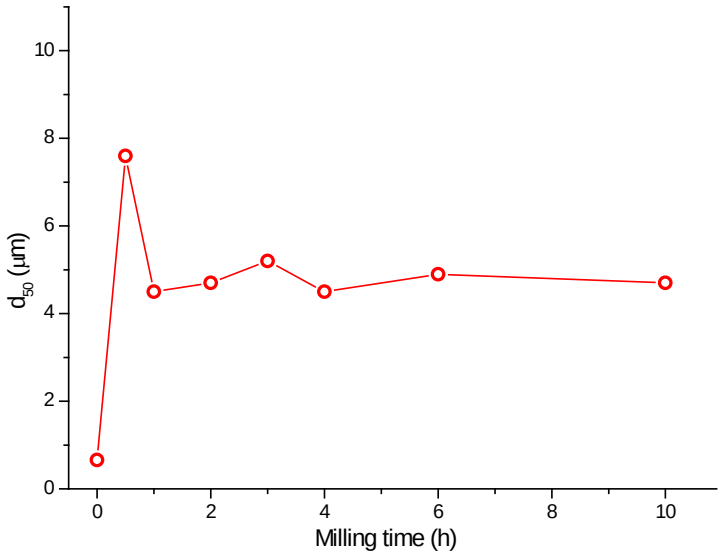

Fig. 10. Evolution of the d50 parameter as a function of the milling time for the S2 samples.

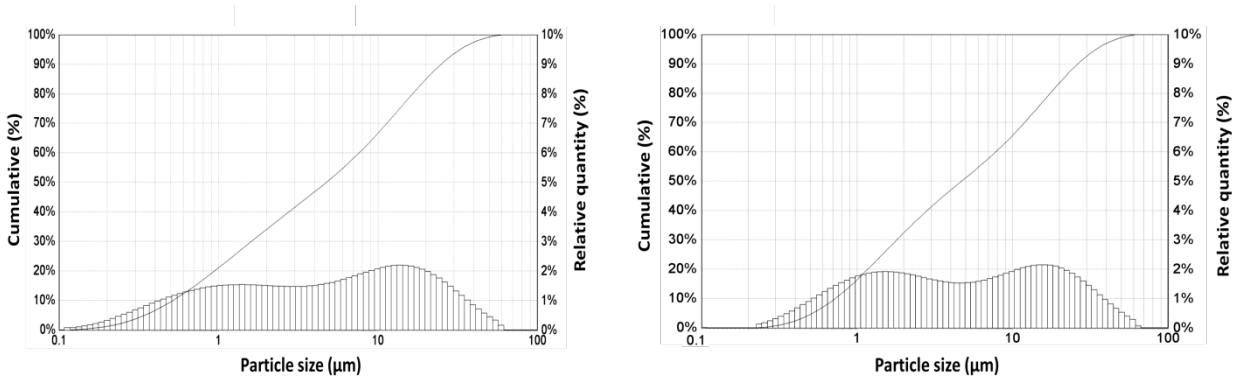

Fig. 11. Particle size distribution of the samples milled for 2 and 10 h in the case of the composition S2 (the cumulative and relative quantity represents vol. %).

The particle size distribution (vol. %) of the samples milled for 2 and 10 h in the case of the composition S2 is shown in Fig. 11. The particles size distribution of these two samples is similar. It can be observed that in both cases the particle size distribution is bimodal. The particle size distribution is in the same manner for all the milling time from 1 to 10 h of milling. The presence of two types of particles is assigned to the two types of process that are present in the milled samples: cold welding and fragmentation. The smaller particles come from the fragmentation of the bigger one and the bigger one is provided by cold welding of the smaller ones. Is assumed that these two types of processes are in a quasi-equilibrium for these milling times and for this composition of the material. The particle size distribution doe not reveal the presence of very fine particles (less than 100 nm), particles that have been evidenced by SEM analyses. It is assumed that the very fine particles are attached by the larger ones and cannot be separate during ultrasound treatment applied in particle size distribution analysis procedure.

Summary

Nanocomposites of the Ni_3Fe/Fe_3O_4 type have been successfully obtained using accessible precursors, Ni, Fe and Fe_2O_3, in various ratios, by high energy reactive mechanical milling. The ratio among starting powders was chosen in such way in order to vary the ratio between Ni_3Fe intermetallic compound and Fe_3O_4 in the final products. The formation of the nanocomposite has been studied by X-ray diffraction technique. By scanning electron microscopy, energy dispersive X-ray spectrometry and laser particle size analysis have been investigated the powder morphology, local chemical homogeneity and particles size distribution. The nanocomposite is forming continuously during the entire period of milling. The nanocomposite formation begins after 2 h of milling in the case of all the compositions. In the case of composition with the highest amount of metallic phases after 10 h of milling the nanocomposite consists in Ni_3Fe and Fe_3O_4. A small amount of unreacted Fe_2O_3 is evidenced. The increase of the amount of oxide in the starting mixtures leads to the formation of a larger amount of magnetite in the final product and also leads to the changes of the phases in composite after the end of milling time. Fe_3O_4, fcc Ni-based structure and unreacted Fe_2O_3 and Fe phases are founded in the nanocomposite with the higher amount of oxide in the starting mixture. The mean crystallite size of the composite main constituent phases, Ni_3Fe and Fe_3O_4, is in the range of 9-12 nm independent on the ratio between the metallic and oxide phases. The particles shape of the nanocomposite has no regular shape. The nanocomposite powder has two types of particles: very fine particles (size less than 100 nm) and large particles (a few micrometers in size). The micrometric particles consist in fine agglomerated and welded particles. The median diameter d_{50} has large variation in the first stage of milling and a small variation on each milling time is evidenced after that.

Acknowledgement

This work was supported by a grant from the Romanian National Authority for Scientific Research, CNCS and UEFISCDI, project number PN-III-P2-2.1-PED-2016-1816.

References

[1] J. Xiang, X. Shen, F. Song, M. Liu, G. Zhou, Y. Chu, Fabrication and characterization of Fe-Ni alloy/nickel ferrite composite nanofibers by electrospinning and partial reduction, Mater. Res. Bull. 46 (2011) 258-261. https://doi.org/10.1016/j.materresbull.2010.11.004

[2] S. Wu, A. Sun, W. Xu, Q. Zhang, F. Zhai, P. Logan, A. Volinsky, Iron-based soft magnetic composites with Mn-Zn ferrite nanoparticles coating obtained by sol-gel method, J. Magn. Magn. Mater. 324 (2012) 3899-3905. https://doi.org/10.1016/j.jmmm.2012.06.042

[3] L.A. Dobrzanski, M. Drak, B. Ziebowicz, New possibilities of composite materials application-materials of specific magnetic properties, J. Mater. Process. Technol., 191 (2007) 352–355. https://doi.org/10.1016/j.jmatprotec.2007.03.029

[4] T. Caillot, G. Pourroy, D. Stuerga, Novel metallic iron/manganeseezinc ferrite nanocomposites prepared by microwave hydrothermal flash synthesis, J. Alloys Compd. 509 (2011) 3493-3496. https://doi.org/10.1016/j.jallcom.2010.12.096

[5] B.D. Cullity, C.D. Graham, Introduction to magnetic materials, second ed., Press&Wiley, New Jersey, USA, 2009.

[6] A. Goldman, Modern ferrite technology, second ed., Springer, Pittsburgh, USA, 2006.

[7] K. Hirota, M. Obatal, M. Kato, H. Taguchi, Fabrication of full-density Mg ferrite/Fe-Ni permalloy nanocomposites with a high-saturation magnetization density of 1 T, Int. J. Appl. Ceram. Technol. 8 (2011) 1-13. https://doi.org/10.1111/j.1744-7402.2009.02477.x

[8] T.F. Marinca, I. Chicinaş, O. Isnard, Structural and magnetic properties of the copper ferrite obtained by reactive milling and heat treatment, Ceram. Int., 39 (2013) 4179-4186. https://doi.org/10.1016/j.ceramint.2012.10.274

[9] T.F. Marinca, H.F. Chicinaş, B.V. Neamtu, O. Isnard, A. Mesaroş, I. Chicinas, Composite magnetic powder of Ni_3Fe/Fe_3O_4 type obtained from $Fe/NiO/Fe_2O_3$ mixtures by mechanosynthesis and annealing, J. Alloys Compd. 714 (2017) 484-492. https://doi.org/10.1016/j.jallcom.2017.04.263

[10] G. Couderchon, Alliages fer-nickel et fer-cobalt e Proprietes magnetiques, Publisher Techniques de l'ingenieur, Traite Genie Electrique, 1994, pp. 1e24. D2 130.

[11] I. Chicinaş, Soft magnetic nanocrystalline powders produced by mechanical, alloying routes, J. Optoelectron. Adv. Mater. 8 (2006) 439-448.

[12] S. Chikazumi, Physics of Ferromagnetism, second ed., Oxford University Press, New York, USA, 1997.

[13] A.L. Patterson, The Scherrer formula for X-ray particle size determination, Phys. Rev. 56 (1939) 978-982. https://doi.org/10.1103/PhysRev.56.978

[14] T.F. Marinca, H.F. Chicinaş, B.V. Neamtu, O. Isnard, I. Chicinaş, Structural, thermal and magnetic characteristics of Fe_3O_4/Ni_3Fe composite powder obtained by mechanosynthesis-annealing route, J. Alloys Compd. 652 (2015) 313-321. https://doi.org/10.1016/j.jallcom.2015.08.249

[15] C.N. Chinnasamy, A. Narayanasamy, N. Ponpandian, K. Chattopadhyay, H. Guerault, J-M Greneche, Magnetic properties of nanostructured ferrimagnetic zinc ferrite, J. Phys.: Condens. Matter. 12 (2000) 7795–7805. https://doi.org/10.1088/0953-8984/12/35/314

[16] C. Suryanarayana, Mechanical Alloying and Milling, Marcel Dekker, 2004. New York, USA. https://doi.org/10.1201/9780203020647